INFLUENCE OF HANDRAIL TYPES ON AERODYNAMICS OF LONG-SPAN BRIDGE DECK

M. N. Haque*

Department of Civil Engineering, Chittagong University of Engineering and Technology, Chittagong, Bangladesh
**Corresponding Author: naimulce@gmail.com*

ABSTRACT
Aerodynamic response is one of the main deign consideration for long-span bridge deck and this is quite sensitive to the shape of the bridge deck. This paper numerically investigates the influence of handrail types such as solid handrail, perforated handrail with curb and without curb on aerodynamic responses of bridge deck with fairing. Edge fairing is attached at the side of the bridge deck to make it more practical and improve the aerodynamic responses. The steady state force coefficients and the flow field were taken as a parameter of interest. It was found that the types of handrail alter the aerodynamic behaviour of the bridge deck noticeably.

Keywords: Deck equipment; handrails; curb; aerodynamic response; bridge deck; CFD

INTRODUCTION
Long span bridges are susceptible to various aeroelastic phenomena under the wind action and in the design stage of the bridge deck, aerodynamic responses are considered as one of main design aspect. Accurate prediction of aerodynamic responses is required to ensure safety and stability of the bridge deck against wind. To obtain the exact responses under wind action, bridge deck should be modelled along with its deck equipments. There are a number of common deck equipments such as handrail, safety barrier, median divider, inspection rails and light post etc attached to the deck. Even though, the size of these deck equipments are small as compared to the deck, their presence will influence the aerodynamic responses as it is already shown that aerodynamic response is a quite sensitive to the shape of the bridge deck (Shiraishi and Matsumoto, 1983 and Larsen and Wall, 2012).

Among these deck equipments, handrail is one the most common and often attached to the deck. Nagao et al. (1997) investigated the effects of perforated handrail on vortex-shedding vibration. They found that the size of the horizontal bars affects the vortex-shedding vibrations significantly. Later, Bruno and Mancini (2002) showed that addition of perforated handrails increases the overall bluffness of the deck by employing Large Eddy Simulation (LES). In previous studies only the perforated handrails were taken into consideration, however, for practical bridges, along with the perforated handrail, solid handrail is also attached. Further, perforated handrails are provided along with the curb or without curb. Therefore, it is required to know how the variation of the handrail types affects the aerodynamic responses due to its practical demand.

In the present study a numerical investigation was carried out by employing Unsteady Reynolds Averaged Navier-Stokes simulation (URANS) to show the influence of handrail types on aerodynamics of bridge deck with edge fairing. Fig.1 shows the cross section of the considered bridge deck. The top and bottom plate slopes of the fairing are set to 40^{o} and 20^{o}, respectively. The side ratio (R) of the bridge deck is maintained at 5 and Reynolds number (R_e) is set to 6.0×10^4. Three different types of handrail namely, solid handrail, perforated handrail with curb and without curb is taken into consideration as shown in Fig.2. The steady state force coefficients and the flow fields are taken into consideration as parameter of interest.

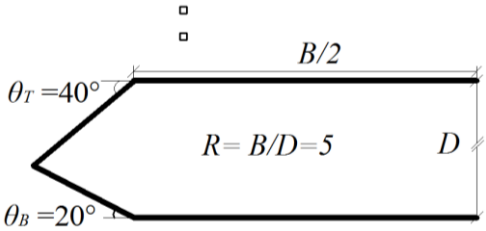

Fig.1: Cross section of the bridge deck (with perforated handrails without curb) considered in the present study

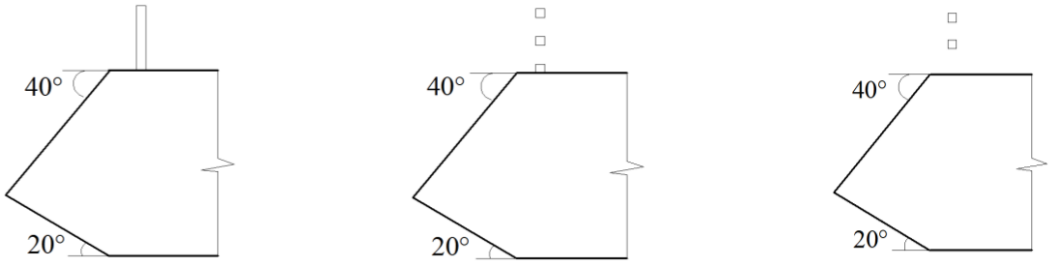

(a) Solid Handrail (b) Perforated handrail with curb (c) Perforated handrail without curb

Fig.2: Types of handrail considered in the present study

NUMERCIAL FORMULATIONS

The ensemble averaged Navier-Stokes equations called unsteady Reynolds-Averaged Navier-Stokes (URANS) equation was used to model the flow around the bridge deck. The flow was assumed to be two-dimensional and incompressible in nature. The governing equations were as follows;

$$\frac{\partial \overline{U}_i}{\partial x_i} = 0 \tag{1}$$

$$\frac{\partial \overline{U}_i}{\partial t} + \overline{U}_j \frac{\partial \overline{U}_i}{\partial x_j} = -\frac{1}{\rho}\frac{\partial \overline{P}}{\partial x_i} + \frac{\partial}{\partial x_j}\left[\nu\left(\frac{\partial \overline{U}_i}{\partial x_j} + \frac{\partial \overline{U}_j}{\partial x_i}\right) - (\overline{u_i' u_j'})\right] \tag{2}$$

where, $\overline{U}_i$ and x_i were the averaged velocity and position vectors respectively, t was the time, $\overline{P}$ was the averaged pressure, ρ was the air density, ν was the fluid viscosity. The turbulence modeling was attained by utilizing the k-ω SST turbulence model (Menter, 1994; Menter et al., 2003). Convective and diffusive terms in the governing equations were discretized with second order accurate central differencing schemes. For time integration second order accurate backward differentiation formulae method was utilized. PISO (Pressure implicit with splitting of operator) algorithm was utilized to solve these discretized equations. An open source code OpenFOAM was used as a solver.

Simulations were performed in a two dimensional domain with 48D in length and 25D in height, where D was the height of the bridge deck section. The object was placed at 18D downstream of the inlet. The outlet boundary was placed at 25D downstream of the object and height of the domain was 25D. The domain was sufficiently large to avoid unnecessary disturbance of the boundary conditions. At the outlet, pressure boundary condition, at the top and bottom of the domain, slip boundary condition and at the body, non-slip boundary condition was implemented. The domain was discretized spatially by a non-uniform structured grid and the cell size was varied gradually with a geometric progression of 1.05 in all directions. Further details of the model, grid system and validation can be found in (Haque et al., 2015a and 2015b).

RESUTLS AND DISCUSSIONS

The mean and rms values of the steady state force coefficients of the considered bridge decks are compared in Table 1. All the force coefficients are normalized with the width of the deck (B). As can be seen the reduction of the solidity ratio of the handrails improves the static aerodynamic responses of the

bridge decks. A trend can be noticed that both the mean and rms value of the force coefficients decreases from solid to perforated with curb and perforated with curb to without curb case. However, the perforated handrail with curb has the highest negative lift force value among the three, which means the deck with this type of handrail has increased stability against wind. Most interestingly, only the absence of the curb has noticeable influence on the force coefficients as reflected in the last column where a comparison was made between the perforated handrail with and without curb cases.

To better understand the responses, the time averaged pressure distributions are plotted in Fig. 3. Various important flow features can be noticed in the pressure field. For the case of perforated handrails without curb, very large suction appears at the leading edge side just before the handrail, after that,

Table 1: Steady state force coefficient comparison of the considered bridge decks

Force coefficients	Solid (1)	Perforated With Curb (2)	Perforated Without Curb (3)	Percentage variation (%)	
				(1) & (2)	(2) & (3)
Mean value of drag force coefficient (C_D)	0.732	0.649	0.553	11.33	13.12
Mean value of lift force coefficient (C_L)	-0.156	-0.246	-0.176	57.69	44.87
Mean value of moment coefficient (C_M)	0.202	0.099	0.051	51.00	23.75
rms value of lift force coefficient (C_L')	0.007	0.002	0.001	71.42	14.29
rms value of moment coefficient (C_M')	0.001	0.0004	0.0002	60.00	20.00

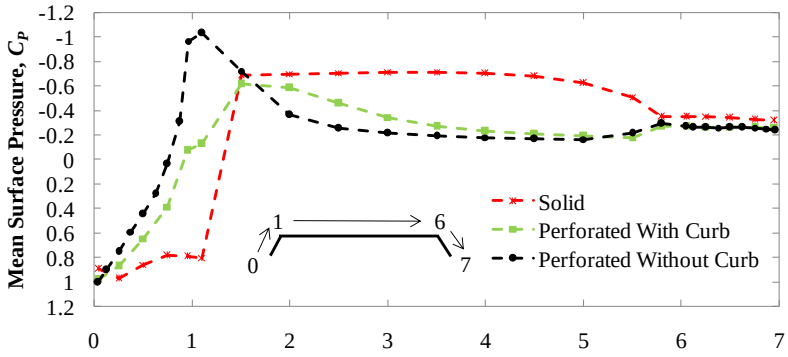

(a) Top surface of the bridge deck

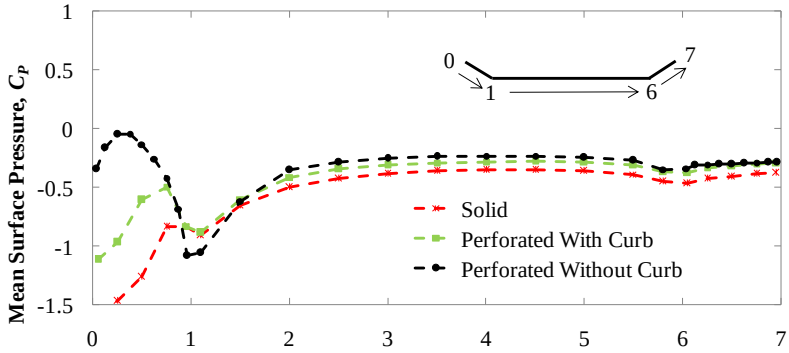

(b) Bottom surface of the bridge deck

Fig. 3: Time averaged pressure distribution around the bridge deck (Contd.)

suddenly pressure recovery occurs at the top surface of the deck. However, reverse phenomenon can be observed for the case of solid handrail case. Similar to the deck top surface, pressure field are mainly affected at the leading edge side of the deck bottom surface. Large suction appears at the leading edge bottom surface of the deck for the cases of solid and perforated handrail with curb. In the case of

perforated handrail without curb the deck has the highest negative lift value, which implies that the pressure distribution at the deck top surface is the influential one as it has the lest magnitude of suction.

The time averaged velocity distribution around the bridge deck for the considered types of handrail are compared in Fig. 4. The observation made earlier is also reflected in the velocity distribution. Large shear layer separation can be noticed both at the deck top surface and leading edge bottom surface. Basically, this separated shear layer creates the suction at the top and bottom surface of the deck. In the all the three cases clear after-body vortex shedding can be seen at the trailing edge side. However, the size of the vortex decreases for the case of perforated handrail with and without cases as compared to the solid handrail case.

CONCLUSIONS

A relative comparison of steady-state aerodynamic characteristics of bridge deck for various handrail types was made. At the current Reynolds number (R_e of 6.0×10^4) and considered geometry (R=5), we found that the types of handrail has noticeable influence on the force-coefficients and flow field. As the solidity ratio of the handrail decreases, the steady-state aerodynamic responses of the bridge deck improve. Even though, the variation in handrail types is made at the top surface of the deck, it affected the bottom surface of the deck pressure and velocity fields as well. Due to the presence of the handrail, the follow separation occurs both the leading and trailing edge side of the deck and depending on the solidity ratio of the handrail, the intensity of separation varies. Therefore, handrail should be properly modelled during the time of numerical and experimental investigation for actual estimation of the aerodynamic responses of the bridge deck.

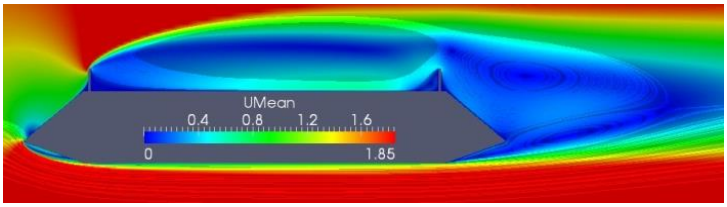

(a) Solid handrail

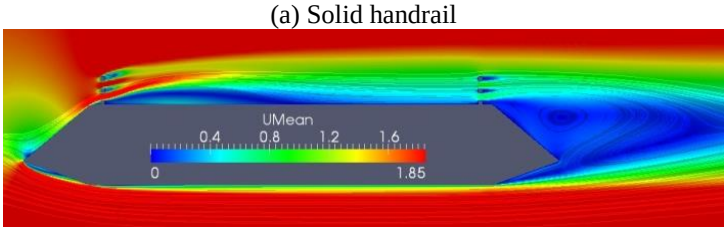

(b) Perforated handrail with curb

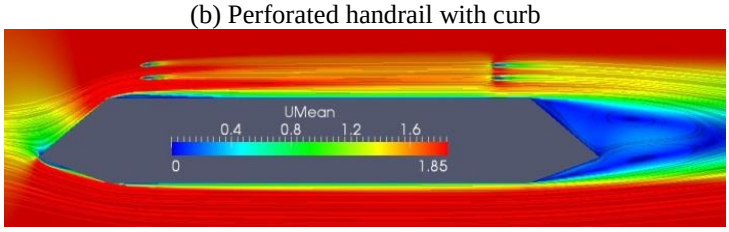

(c) Perforated handrail without curb

Fig.4: Time average velocity distribution around the bridge deck

REFERENCES

Bruno, L and Mancini, G. 2002. Importance of deck details in bridge aerodynamics. *Structural Engineering International*, 12(4):289-294.

Haque, MN, Katsuchi, H, Yamada, H and Nishio, M. 2015a. Strategy to develop efficient grid system for flow analysis around two-dimensional bluff bodies. *KSCE Journal of Civil Engineering*, 20(05): 1-12.

Haque, MN, Katsuchi, H, Yamada, H and Nishio, M. 2015b. Flow field analysis of a pentagonal-shaped bridge deck by unsteady RANS. *Engineering Application of Computational Fluid Mechanics*, 10(1): 1-16.

Larsen, A, and Wall, A. 2012. Shaping of bridge girders to avoid vortex shedding response. *Journal of Wind Engineering and Industrial Aerodynamics*, 104-106: 159-165.F.R.
Menter, F. 1994. Two-equation Eddy-viscosity Turbulence Model for Engineering Applications. *AIAA Journal*, 32:1598–1605.
Menter, FR, Kuntz, M and Langtry, R. 2003. Ten years of industrial experience with the SST turbulence model. *Proceedings of Turbulence, Heat and Mass Transfer* 4, 12-17, October, Antalya, Turkey, 625–632.
Shiraishi, N, and Matsumoto, M. 1983. On classification of Vortex-Induced oscillation and its application for bridge structures. *Journal of Wind Engineering and Industrial Aerodynamics*, 14: 419–430.
Nagao, F, Utsunomiya, H, Yoshioka, E, Ikeuchi, A and Kobayashi, H. 1997. Effects of handrails on separated shear flow and vortex-induced oscillation. *Journal of Wind Engineering and Industrial Aerodynamics*, 69-71: 819-827.